Journal of Advances in Radiology and Medical Imaging
Volume 6 | Issue 1
ISSN: 2456-5504

Research Article Open Access

Global Correction of $T1_0$ Non-uniformity in mMR Breast Coil with Multiple Tube Phantom-based Technique and its Validation in Breast MRI: a Feasibility Study

Negi PS[*1,2], Mehta SB[1,2] and Jena A[1,2]

[1]PET SUITE: House of Diagnostics and Indraprastha Apollo Hospitals, Department of Molecular Imaging and Nuclear Medicine, Indraprastha Apollo Hospitals, Sarita Vihar, Delhi-Mathura Road New Delhi, India

[2]Department of Physics, Vivekananda Global University, Sector 36, Sisyawas, NRI Road, Jagatpura, Jaipur, Rajasthan, India

[*]**Corresponding author:** Negi PS, M.Sc., Department of Molecular Imaging and Nuclear Medicine, PET SUITE, Indraprastha Apollo Hospitals, SaritaVihar, Delhi–Mathura Road, New Delhi 110076, India, Tel: +91-9958798794, E-mail: pradeepnegi1979@gmail.com

Citation: Negi PS, Mehta SB, Jena A (2021) Global Correction of $T1_0$ Non-uniformity in mMR Breast Coil with Multiple Tube Phantom-based Technique and its Validation in Breast MRI: a Feasibility Study. J Adv Radiol Med Image 6(1): 105

Abstract

Background: Non-uniform native T1 ($T1_0$) distribution influences reliable measurement of K^{trans}: a pharmacokinetic parameter (K^{trans}) that quantitatively measures neovascularization of the tumor tissue that has been used for the classification of malignant breast lesions and to monitor therapy response.

Purpose: To develop a method to assess spatial inhomogeneity of native $T1_0$ relaxation time in dedicated mMR breast coil and adopt corrective measure to normalise native $T1_0$ values of breast tissue.

Methods: In-house designed multiple tube phantoms, containing gadolinium (Gd) solution were placed in breast coil cuffs which fill the cuff space.

$T1_0$ at various spatial locations was calculated by applying dual flip angle (2^0 and 15^0) image protocol. The correction factors were derived from the deviation of $T1_0$ value from centrally placed phantom in each breast coil to achieve global $T1_0$ homogeneity. The calculated $T1_0$ values were normalized by applying correction factors. Correction factor so derived was applied in 46 patients who were undergoing screening MRI and turned out to be normal, to assess its effect on the spatial distribution of $T1_0$ value in fat and fibroglandular tissue in the breast.

Results: Post correction, greater homogeneity was achieved with in the breast coil space with uniformity of $T1_0$ distribution in phantom at different spatial location (P value: 0.091 corrected vs 0.00049 uncorrected); and the breast tissue with P value for glandular tissue 0.542 and fat 0.414 post correction vs 0.0003* and 0.00001* pre correction respectively).

Conclusion: Significant homogeneity of $T1_0$ distribution in normal breast tissues can be achieved by applying correction factors derived with multiple tube phantom-based technique.

Keywords: DCE-MRI; Native T1 ($T1_0$); Uniformity; mMR Breast Coil; Multiple Tube Phantom

List of abbreviations: GD: Gadolinium; DCE-MRI: Dynamic Contrast Enhanced-Magnetic Resonance Imaging; PK: Pharmacokinetic; RF: Radiofrequency; FOV: Field of view; DFA: Dual Flip Angle; mMR: Molecular Magnetic Resonance; MRI: Magnetic Resonance Imaging; PET/MRI: Positron emission/ Magnetic Resonance Imaging; Gd-DTPA: Diethylenetriamine pentaacetic acid gadodiamide; ROI: Region of Interest; VIBE: Volume interpolated body examination; ms: Milliseconds; mm: Millimetres; MPR: Multiplanar reformation; VFA:Variable flip angle; IR: Inversion recovery

Introduction

Breast cancer is the most commonly diagnosed cancer in females [1]. Dynamic Contrast Enhanced-Magnetic Resonance Imaging (DCE-MRI) of Breast provides morphological and angiogenic information which is helpful to differentiate between benign and malignant tissue [2-4]. This technique acquires T_1-weighted images prior and post administration of Gadolinium (Gd) contrast agent which provides microvascular properties of the tumor tissue, by calculating time varying signal intensity curvesThese time varying signal intensity curves in routine DCE-MRI derived from high spatial resolution but low temporal resolution images acquired in order of a minute or so Lesions can be differentiated into three types based on time intensity curves; 1) Wash in and wash out (curve type 3) denoting malignant characteristic, 2) Initial rise and Plateau (curve type 2) denoting indeterminate: either benign or malignant characteristic, and 3) Persistent rise (curve type 1) denoting benign characteristic [5-11].

High temporal resolution DCE-MRI with few seconds per frame enables quantitative pharmacokinetic (PK) modeling of contrast agent uptake [12]. However, PK parameters is influenced by $T1_0$ (msec) and at the same time $T1_0$ is influenced by several extrinsic factors including nonlinear RF amplifier due to RF-inhomogeneity, incorrect power setting of 90^0 pulse, distortions in slice profile, B1 inhomogeneity and flip angle used in MR sequence. B1 inhomogeneity is known to be more critical in higher field strengths e.g. at 3.0T B1 variations across the breasts of patients have been reported around 33%–40% [13, 14]. Kuhl et al. observed in their study that the presence of B1 inhomogeneity was due to the large field-of-view (FOV) and the off-centered positioning of patients. They reported significant differences in B1 values across the FOV between right and left breast. The reduction in intensity of contrast enhancement in breast tissue had also been reported with reduction in B1 [15].

B1 inhomogeneity is known to effect accurate calculation of PK parameters [16]. B1 inhomogeneity observed across the FOV, affects the actual flip angle (i.e. flip angle error) and finally leads to substantial variations in the value of $T1_0$ across the breasts. Studies have reported multiple methods to homogenize the magnetic field by adapting specialized coils, shimming based technologies or by the correction of B1 map [17-20].

Bedair R et al, 2016 [18] used the B1 mapping method for inhomogeneity correction which was subsequently used for calculation of native $T1_0$ maps first without B_1 correction and then after B_1 correction on a 3T system. This study signified the importance of correcting B1 so that error should not be translated in subsequent analysis of PK.

We adopted an innovative method to homogenize the physical space with the help of in-house designed multiple tube phantom using DFA (Dual Flip Angle) protocol.

The $T1_0$ values were normalized in the mMR breast coil-cuff by applying correction factors derived for each spatial location by using multiple tube phantom placed in each coil cuffs as external standards

The current work has been designed to note the pattern of $T1_0$ inhomogeneity, and to see the influence of the spatial correction at multiple locations to achieve global homogeneity in the mMR breast coil for the validation in breast MRI patients.

Material and Methods

This study was performed on simultaneous PET/MRI Biograph mMR (Siemens, Erlangen, Germany) by using mMR breast coil (4 channels). We had used prototype in-house designed multiple tube (19 tubes) phantom for each side of breast coil-cuffs. These multiple-tube phantoms were placed to fill the imaging field of dual breast coil cuffs to measure $T1_0$ values in various planes, which was used for global $T1_0$ normalization across the coil. Our patient group consists of 46 women (mean age 49 years, range 31 to 77 years: 26 premenopausal and 22 post premenopausal) who had undergone screening DCE-MRI between January 2018 to October 2019 and reported to have no breast lesion. The study protocol was approved by the ethics body of the institute and consent of all participating patients was taken.

Phantom Creation

Phantom tubes were filled with contrast solution i.e. water and Gd-DTPA [(diethylenetriamine pentaacetic acid gadodiamide {Omniscan}); 0.1 mMol] mixed in the ratio of 10:1 [19]. Each phantom contains 19 tubes, which were arranged in 5 rows containing 3,4,5,4 and 3 tubes in 1, 2, 3, 4 and 5 rows respectively. The dimension of the tube was 16cm x 4cm (length x diameter) and each tube was at a gap of 2cm on a porous thermocol support surface. The arrangement of tubes was done in this manner, so that phantom would be best fitted in the breast coil. These phantoms were placed vertically in each cuff so that tubes would fully occupy cuff space of the breast coil (Figure 1).

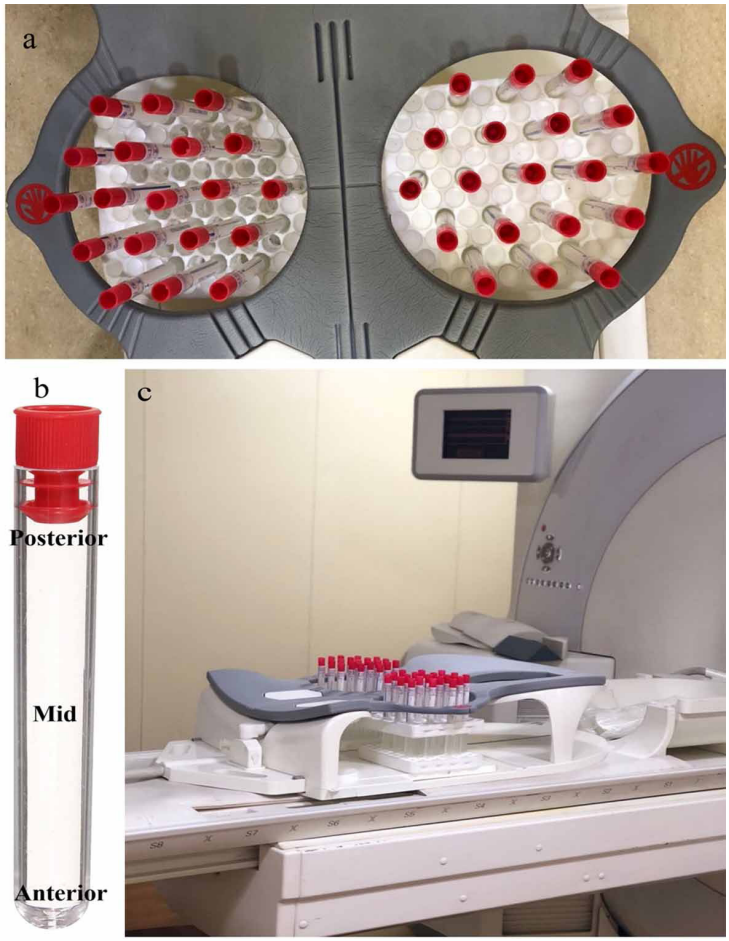

Figure 1: a) In multiple tubes phantom, tubes were filled with GD and arranged as 3,4,5,4 and 3 tubes per row respectively; b) the anterior, middle and posterior part of the phantom tube and c) multiple tube phantom filling the space of breast coil cuffs in Siemens Biograph mMR System

Data Acquisition and imaging protocol

Multiple tube phantoms were placed in breast coil cuffs which fill the cuff space, and positioned corresponding to the isocenter of the magnet using light localizer. After localizer images obtained in all three coordinates, 2^0 flip angle proton density and 15^0 flip angle non-fat-suppressed T1 weighted images (VIBE-Volume interpolated body examination) were acquired for native $T1_0$ calculation for phantom experiment TE (Time to Echo) 1.8 ms, TR (repetition time) 5.2 ms, FOV 360 mm, slices 36, TA (acquisition time) 20.7s, resolution 256 x 256 and voxel size 4.4 mm×1.4 mm×4.0 mm. [21, 22]. $T1_0$ at various spatial locations calculated by using DFA protocol was normalized to achieve global $T1_0$ homogeneity, by applying correction factors at each spatial location. These correction factors were derived by calculating the deviation of $T1_0$ value at a spatial location from centrally placed voxels of the phantom in each breast coil. The derived correction factors was applied to 46 normal breast MRI cases to assess the distribution of $T1_0$ values in fat and fibroglandular tissues before and after $T1_0$ correction. MRI protocols were performed in a fix table position for phantom study and

patient's study. Matrix size of phantom study was kept same as patient's study. For technical reason, the phantom scans were acquired in coronal plane and the patients scan were in axial plane covering both breasts completely.

Region of Interest (ROI) Creation and data compilation

The ROI's were manually drawn over each tube on both the multiple tube phantoms on the 15^0 flip angle images (number of pixels: 44/ area: 0.22sq/cm) and these ROI's were copy pasted on 2^0 flip angle images across all 36 slices.

The $T1_0$ values were calculated by putting the intensity values of both the ROI's (one from 2^0 and another from corresponding spatial location from 15^0 flip angle images) on an excel sheet.

Matching the ROIs of phantom and ROIs on corresponding spatial location on breast images was a critical step in our study as it requires correct placement of ROI on corresponding spatial location on breast images to derive accurate image intensity for $T1_0$ calculation for the purpose of clinical validation.

Image processing

For the evaluation of $T1_0$ values, the non-fat-suppressed T1 weighted pre-contrast 2^0 and 15^0 flip angles VIBE series were separately evaluated in phantom and patients. The Native $T1_0$ was calculated with the help of equation 1, 2 manually on the excel sheet [23].

Equation1 $$T_{10}^{-1} = \frac{1}{TR}\ln\left[\frac{S_R Sin\alpha 2 Cos\alpha 1 - Sin\alpha 1 Cos\alpha 2}{S_R Sin\alpha 2 - Sin\alpha 1}\right]$$

Equation 2 $$S_R = \frac{S_{\alpha 1}}{S_{\alpha 2}}$$

$S_{\alpha 1}$ = intensity value at α1 (2^0 flip angle), $S_{\alpha 2}$ = intensity value at α2 (15^0 flip angle), TR= Repetition time, In= Natural Log

As patient's data was acquired in axial planes and phantom data in coronal planes; therefore, the patient's images of 2^0 and 15^0 flip angles were reformatted and post processed in coronal planes using MPR (Multiplanar reformation) in Syngovia (Siemens) workstation to match patient's data with the Phantom Data. ROIs were drawn on the 15^0 flip angle image on visible fatty and normal fibroglandular tissue on breasts for all patients randomly at different locations. The same ROI was copied and pasted on corresponding 2^0 flip angle images at the same location for calculation of native $T1_0$. Both patient and phantom study were spatially synchronized by using Syngovia software for normalizing the $T1_0$ at every spatial location in patients. In 2^0 and 15^0 flip angle images, intensity values of the fat and fibroglandular tissue in the breast were manually put in an excel sheet and $T1_0$ were measured (Figure 2).

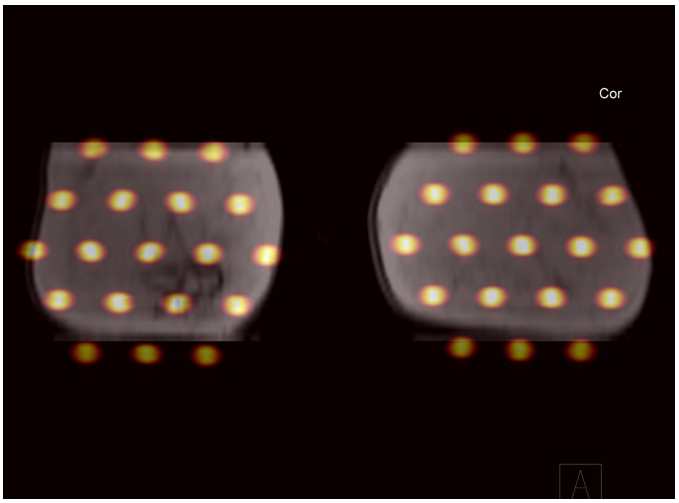

Figure 2: Both patient and phantom study was spatially synchronized by using Syngovia software

Reference native $T1_0$ in phantom study

As a first step, the mean $T1_0$ value of multiple tube phantoms at the center of each coil cuffs were measured as 6.29± 0.22 ms; which was taken as reference to find a deviation factor for each spatial location. Variations in $T1_0$ value was documented for each breast coil from latero-medial, antero-posterior and cranio-caudal directions on each side, before and after applying the necessary correction factor to assess achieved normalization.

Correction Factor

Inhomogeneity in $T1_0$ distribution was noted for bilateral breast coils in the phantom study. This inhomogeneity was corrected by applying a correction factor for each ROI locations using the following equation

Equation 3

$$Cf_n = \frac{Pht1 - t1_n}{Pht1}$$

$t1_n$ =Measured $T1_0$ Value of phantom, $Pht1$ = $T1_0$ value (6.29± 0.22 ms) of reference phantom, Cf_n = Correction Factor at each spatial location, n= Multiple tube phantom (1, 2,….19)

The formula used for correcting the $T1_0$ value

Equation 4

$$Ct1_n = UCt1_n + (UCt1_n * Cf_n)$$

$Ct1_n$ = Corrected $T1_0$, Cf_n = Correction Factor, $UCt1_n$ = uncorrected $T1_0$

Statistical analysis

Two tail T-test was performed between corrected and non-corrected $T1_0$ value at every spatial location of the breast coil for both phantom and patient's study (fat and fibroglandular tissues). The statistical analysis was performed using the MedCalc statistical software package (version 19.8- 64 bit; Windows Vista/7/8/10).

Results

Phantom study

A significant difference in $T1_0$ values was observed across ROIs between right & left side of breast coil (p values 0.00049) in phantom study. After correction, a convergence of mean $T1_0$ value with regression of standard deviation (SD) was observed suggesting no significant difference (p value 0.091) across spatial locations in the coils. The mean $T1_0$ value before correction was 6.08±1.02 ms and 5.38±1.06 ms in right and left breast respectively, which after correction was changed to 6.12±0.26 ms and 6.03±0.28 ms. A detailed distribution of $T1_0$ values in breast coil was given in Table 1 and Figure 3.

	Un-Corrected T1 values(msec)		Corrected T1 values(msec)	
Tube No.	Right	Left	Right	Left
1	6.79	5.54	6.25	6.20
2	6.24	6.38	6.29	6.29
3	4.80	5.80	5.94	6.25
4	6.80	5.99	6.25	6.28
5	6.85	7.08	6.24	6.19
6	6.71	6.82	6.26	6.24
7	4.77	6.25	5.92	6.29
8	7.08	5.29	6.19	6.13
9	7.61	6.90	6.01	6.23
10	7.07	7.33	6.19	6.12
11	5.98	7.36	6.27	6.11

	Un-Corrected T1 values(msec)		Corrected T1 values(msec)	
Tube No.	Right	Left	Right	Left
12	4.19	5.42	5.59	6.17
13	7.59	5.92	6.02	6.27
14	7.34	6.63	6.11	6.27
15	6.79	7.09	6.25	6.19
16	5.48	6.71	6.19	6.26
17	6.34	5.17	6.29	6.09
18	6.33	5.74	6.29	6.24
19	5.12	6.31	6.07	6.29
20	6.24	4.76	6.29	5.92
21	6.18	4.72	6.29	5.90
22	5.19	4.45	6.10	5.75
23	6.44	5.39	6.29	6.16
24	7.01	5.60	6.21	6.21
25	5.75	5.88	6.24	6.26
26	4.71	5.51	5.89	6.19
27	7.34	5.18	6.12	6.09
28	6.76	6.56	6.26	6.28
29	7.05	6.01	6.20	6.28
30	5.73	5.68	6.24	6.23
31	3.13	4.52	4.70	5.79
32	6.89	5.29	6.23	6.13
33	7.01	5.50	6.21	6.19
34	6.26	4.97	6.29	6.01
35	4.48	5.17	5.77	6.09
36	6.27	4.62	6.29	5.85
37	5.83	5.21	6.26	6.10
38	4.14	5.50	5.56	6.19
39	6.69	5.02	6.26	6.03
40	6.36	4.23	6.29	5.61
41	6.79	4.63	6.25	5.85
42	5.98	5.96	6.27	6.27
43	5.69	4.46	6.23	5.76
44	5.87	4.65	6.26	5.86
45	7.09	5.55	6.19	6.20
46	4.91	7.26	5.99	6.14
47	6.10	5.23	6.28	6.11
48	4.45	3.59	5.75	5.13
49	6.93	5.09	6.22	6.06
50	8.08	4.69	5.78	5.88
51	5.22	3.80	6.11	5.31
52	5.10	3.68	6.06	5.20
53	4.86	4.24	5.96	5.62
54	7.16	4.79	6.17	5.93
55	5.49	2.98	6.19	5.55
56	5.32	3.43	6.14	5.99
57	6.30	3.02	6.29	5.59
Mean	6.08	5.38	6.12	6.03
SD	1.02	1.06	0.26	0.28
P value	0.00049		0.091	

Table 1: The distribution of $T1_0$ values in multiple tube phantom before and after correction at different spatial location in breast coil for both sides

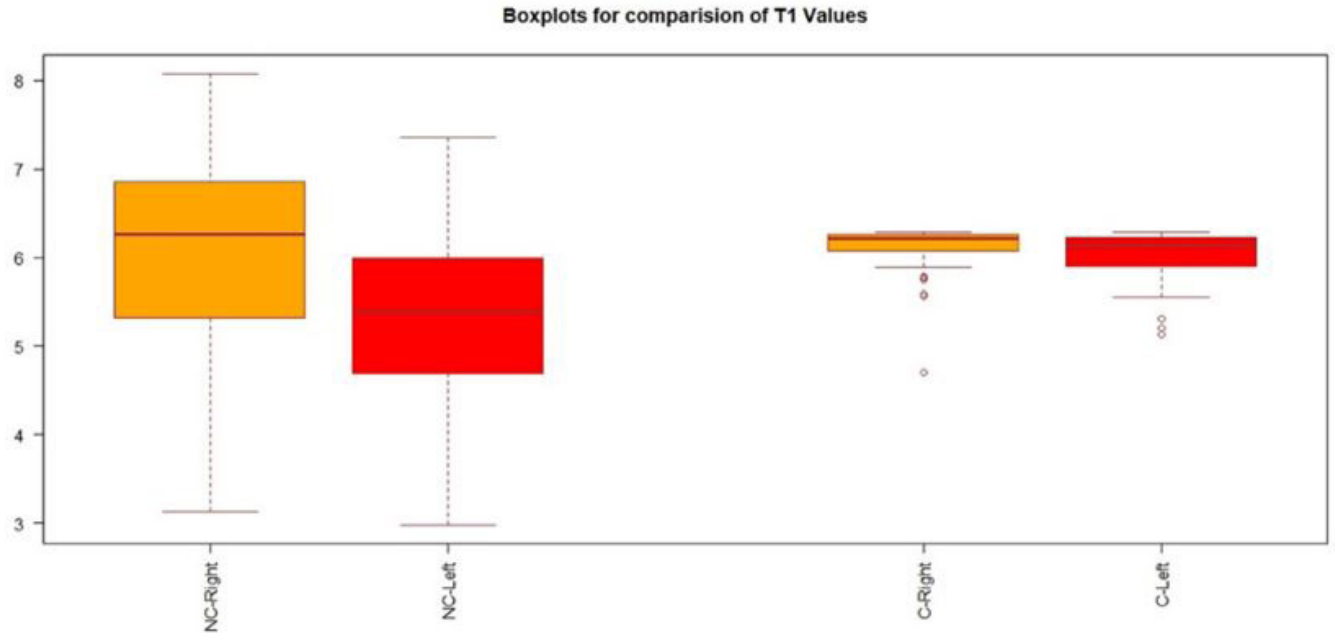

Figure 3: Box plot of uncorrected (NC) and Corrected (C) $T1_0$ value distribution of GD phantoms in both breast cuffs

Patient's studies and validation

A significant difference in mean $T1_0$ values in fat and fibroglandular tissue was observed between right and left sides of the breast coil before correction. Following correction, no significant difference in $T1_0$ relaxation time at different spatial locations was noted. In normal fibroglandular tissue, the mean $T1_0$ value before the correction was 1552.79±684.46 ms and 1007.81±420.13 ms in right and left breast respectively, which after the correction was changed to 1418.98±483.67 ms and 1386.17±482.60 ms. For fat tissue, the mean $T1_0$ was changed from 398.67±47.37 ms and 326.90±93.40 ms to 388.30±9.41 ms and 390.33±13.91 ms for right and left breast respectively after correction. There was no significant difference in the corrected $T1_0$ values of fat tissue (p value 0.41) and fibroglandular tissue (p value0.54) of the right and left breast (Table 2, Figures 4 and 5).

Discussion and Conclusions

Reliable estimation of native $T1_0$ of tissue under investigation is a prerequisite for accurate measurement of pharmacokinetic parameters. This assumes importance because of increasing application of PK parameters to assess the neoangiogenesis property of cancer and in particular its application in breast cancer diagnosis [13,14,17]. One major challenge for mitigating non-uniformity of $T1_0$ distribution is inhomogeneity of radiofrequency transmitted field (B1) [18], its influence on VFA (variable flip angle) which causes substantial deviation (≈52%) in the $T1_0$ value of fat. Nonuniformity of the B1 at 3T has been reported to affect $T1_0$ measurement across the breasts and pose as a challenge for use in quantitative DCE-MRI [24]. Bedair R et al, 2016 [18] also highlighted the influence of B1 at the spatial variation in flip angle across the FOV in a 3T system that is particularly relevant to PK analysis. Development of specially designed volume coils and the use of B1-insensitive adiabatic pulses [25] have demonstrated a substantial effect on the results of quantitative DCE analysis of breast tissue at 3 T [18]. These methods can be specific to a vendor or require specialized software [17-20]. Tsai et al 2017 [17] reported the variations of the average flip angle as 119% and 97% in left breast and right breast respectively, with an overall 22% difference between the two sides on 1.5-T MRI. They used with and without computed B1 corrected VFA to correct $T1_0$ value and compared pre-contrast $T1_0$ relaxation time in fat and breast tumors.

	UC GT T1(msec)		C GT T1(msec)		UC Fat T1(msec)		C Fat T1(msec)	
	Right	Left	Right	Left	Right	Left	Right	Left
1	1703.91	1511.26	1460.54	1446.14	394.27	363.25	373.72	380.38
2	774.69	550.73	764.73	769.34	350.64	345.57	381.90	388.60
3	1985.58	1285.73	1538.76	1538.03	386.25	332.90	390.92	398.05
4	667.67	475.22	659.09	663.86	406.49	348.56	383.06	394.31
5	1620.75	1498.11	1605.58	1620.39	352.99	332.22	398.65	405.24
6	2173.91	1608.68	2145.95	2167.43	473.06	310.57	394.46	398.86
7	681.88	1141.61	1054.30	1092.42	333.24	327.38	392.89	387.22
8	1923.71	1104.26	1426.35	1476.98	329.20	245.83	394.41	375.47
9	1236.72	700.60	1184.11	985.31	313.09	243.64	391.81	362.59
10	1294.17	682.91	1197.78	1043.07	388.68	297.58	393.39	381.14
11	1445.67	1430.20	1432.14	1494.15	373.01	261.62	405.18	389.34
12	1450.88	848.37	1284.45	1252.14	343.05	308.55	381.95	380.40
13	2267.71	1366.46	1808.16	1846.17	359.19	283.90	405.13	388.99
14	3414.93	1455.28	1549.85	1523.91	409.67	287.41	380.17	387.24
15	1445.43	1319.47	1600.99	1626.74	361.38	311.43	393.59	390.60
16	1638.69	1418.55	1544.81	1592.42	343.83	304.49	405.37	396.88
17	429.88	518.95	556.85	589.33	385.06	304.44	393.14	386.64
18	2345.13	1377.66	1933.87	1924.52	374.45	306.58	385.49	374.58
19	1725.40	466.54	1250.31	712.58	351.02	256.97	401.96	382.42
20	864.09	449.74	769.74	686.92	418.70	313.35	382.15	391.41
21	1297.20	802.67	1189.75	1150.07	371.47	315.11	388.40	377.72
22	1381.18	685.69	1176.27	1047.32	436.12	298.99	389.42	389.70
23	959.44	1280.86	1131.17	1178.35	341.22	343.88	390.36	390.75
24	3354.35	1406.06	2487.11	2075.26	522.22	335.05	395.29	400.80
25	2307.16	1486.32	1831.25	1858.03	461.53	289.57	390.10	390.15
26	1343.63	1365.45	1326.35	1359.12	428.67	373.13	381.58	399.45
27	446.96	573.95	485.59	516.47	437.87	311.94	373.65	376.57
28	1613.30	1602.57	1707.13	1746.54	396.36	351.22	381.95	399.09
29	1015.40	1221.65	1250.59	1240.93	341.11	292.69	390.61	391.49
30	1298.82	1539.51	1623.34	1683.77	392.74	365.68	387.40	395.59
31	2457.37	2149.68	2353.52	2431.84	398.17	394.97	394.44	405.66
32	1736.94	945.44	1663.04	1444.05	462.31	327.99	390.75	389.87
33	2597.19	1383.24	2195.22	2041.58	370.61	293.32	365.95	373.60
34	1622.16	992.23	1413.88	1377.28	396.86	320.16	383.63	400.12
35	2111.79	1425.81	2083.09	2065.23	413.92	302.56	383.09	397.02
36	1683.74	1507.27	1801.90	1847.94	477.63	279.45	363.25	377.55
37	1245.96	855.62	1234.30	1187.66	403.27	288.09	380.38	378.04
38	872.38	461.16	807.40	667.97	380.08	346.45	384.68	396.17
39	1895.63	905.24	1762.49	1336.08	363.02	905.24	394.32	458.45
40	1539.70	1141.13	1342.00	1399.05	485.26	271.42	400.16	397.86
41	1958.51	1636.82	1854.17	1851.67	419.78	307.46	374.82	394.83
42	1909.47	1218.05	1828.24	1738.71	463.39	273.17	396.35	381.61
43	544.71	561.58	642.21	732.51	420.70	345.32	396.45	398.82
44	888.46	826.60	981.89	1017.25	429.62	355.13	380.77	387.87
45	1707.04	1357.30	1685.56	1670.37	459.38	321.56	388.28	378.32
46	549.14	417.12	647.43	586.97	418.33	341.66	386.69	388.04
Mean	1552.79	1107.81	1418.98	1376.17	398.67	326.90	388.31	390.34
SD	684.47	420.14	483.67	482.61	47.38	93.41	9.41	13.91
P Value	0.0003*		0.542		0.00001*		0.414	

UC GT $T1_0$: Uncorrected fibroglandular tissue $T1_0$ value; C GT $T1_0$: Corrected fibroglandular tissue $T1_0$ value; UC Fat $T1_0$: Uncorrected Fat $T1_0$ value value; C Fat $T1_0$: Corrected Fat $T1_0$ value

Table 2: The distribution of $T1_0$ values before and after correction in fibroglandular tissue and fat in breast coil for both sides

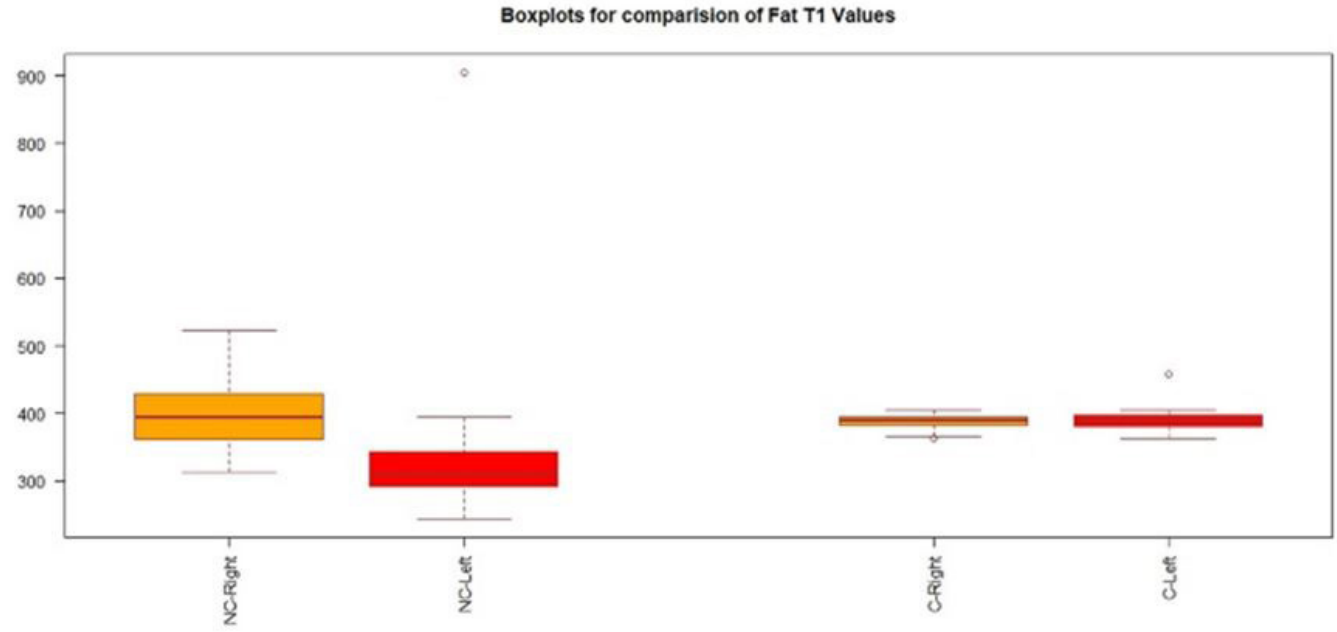

Figure 4: Box plot of mean $T1_0$ values uncorrected (NC) and Corrected (C) $T1_0$ value in fat tissue comparison in both breasts

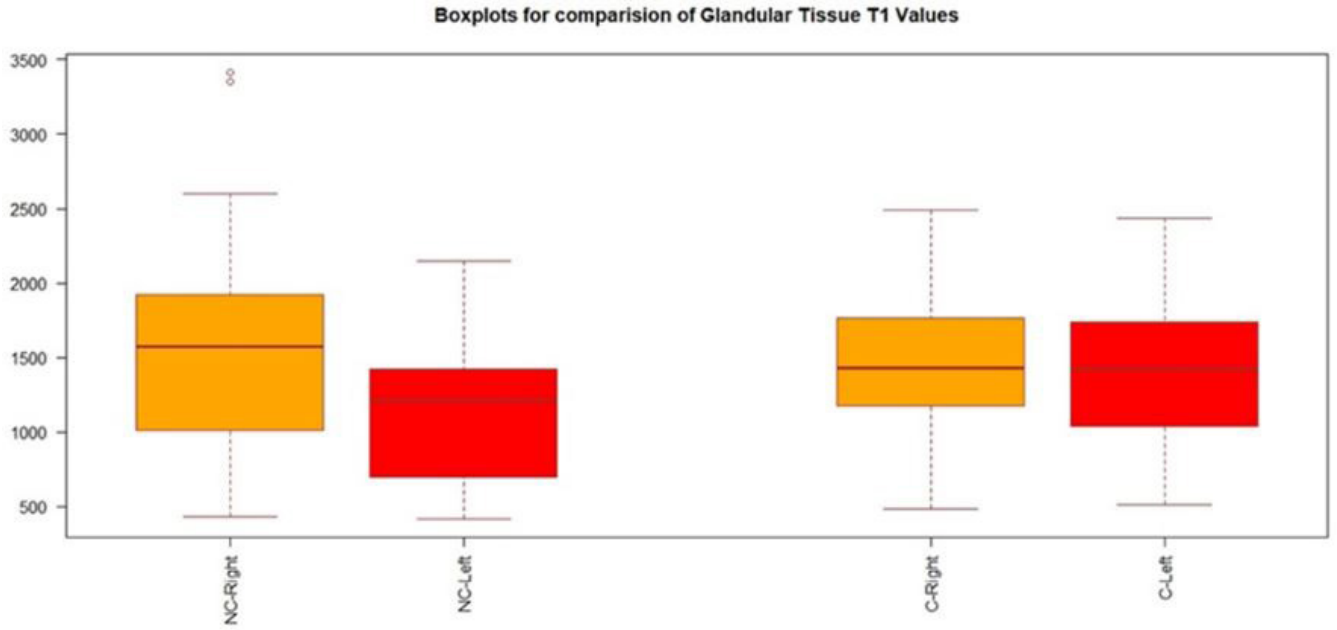

Figure 5: Box plot of mean $T1_0$ values uncorrected (NC) and Corrected (C) $T1_0$ value in normal fibroglandular tissue comparison in both breasts

Pineda et al. (2016) [19] used VFA and multi-inversion recovery (IR) method with reference tissue method and showed accurate B1 map on phantom data. The pharmacokinetic modelling techniques were used to calculate native $T1_0$ of the phantom at voxel based spatial positions. Before B1 correction, the average absolute difference between VFA and IR values was 58% ± 21% ($p < 0.05$); that reduced to 8.1% ± 7.8% ($p > 0.05$) post correction. In the voxels with maximum difference (10% to the maximum) obtained after correction, the average values estimated to be 170% ± 53% without B1 correction that significantly decreased to 28% ± 13% after correction.

In order to circumvent externous and machine hardware impact, in an innovative approach Jena et al. 2013 [21, 22] attempted to correct $T1_0$ by using a single phantom for correction of breast coil. However, this study had an inherent limitation as it uses a single tube phantom for global normalization of $T1_0$. In the current study, an ensemble of 19 tubes was used to make the single phantom, which was used to fill the whole cuff space. This enabled us to generate correction factors for each spatial location in the cuff space that makes the technique more robust. The DFA protocol containing 2^0 and 15^0 flip angles for native $T1_0$ estimation both for phantom experiment and patient's study, provided better correlative evaluation of the patient data.

We have demonstrated on the phantom study, the effects of $T1_0$ normalization on the uniformity of $T1_0$ distribution of bilateral breast coil cuffs showing the convergence of mean $T1_0$ values across the breast coils with significant improvement in correlation between both sides of coils (p value 0.00049 before correction to 0.091 after correction).

This finding was further verified in 46 clinical cases. The influence of $T1_0$ normalization in achieving uniformity of $T1_0$ distribution and effect of normalization on mean $T1_0$ values in fat and fibroglandular tissue of normal breasts at various spatial locations in bilateral breast coils were studied. Fat is known to be an ideal $T1_0$ reference tissue for breast imaging with limited variability [26, 27]. Sung et al. [27] reported the $T1_0$ value of fibroglandular tissue on right and left breast to be 1262.8 ± 37.2 ms, 1304.0 ± 104.5 ms respectively at 3.0 T and mean $T1_0$ value of 367 ± 18 ms for breast fat with VFA using GRE sequence in 6 patients. Similar results for $T1_0$ value for fat and glandular tissues of healthy breasts at 3T have also been reported: 367 ms ± 8 ms and 1445 ± 93 ms respectively in a study of 5 normal breast [28] and 423 ± 12 ms and 1680 ± 180 ms respectively in 6 normal breasts [29], both studies used IR sequence.

The mean native $T1_0$ value of the fat tissue and fibroglandular tissue calculated in our study using DFA technique across bilateral breasts following normalization was also found to be in concordance with above reported values [26, 27 and 28]. In addition, we also achieved significant homogeneity in the $T1_0$ values for fat and glandular tissue at various spatial locations across different regions of breasts and between both breasts with improved p values.

In summary, significant inhomogeneity in the value of $T1_0$ distribution exists between right and left breast coils that can be normalised by using the multiple tube phantom technique adopted in the current study and its portability for application in breast MRI cases. Our findings in normal breast cases are encouraging and with further validation may potentially help improving PK parameters quantification in disease conditions.

Acknowledgement

We thank Department of Physics, Vivekananda Global University, Jaipur, Rajasthan allowing to carry out this research work as part of the Ph.D. thesis program.

References

1. World Health Organizations (2020) World Health Organizations Global Cancer Observatory, Geneva, Switzerland.

2. Schnall MD, Blume J, Bluemke DA, DeAngelis GA, DeBruhl N, et al. (2006) Diagnostic architectural and dynamic features at breast MR imaging: multicenter study. Radiology 238: 42-53.

3. Kuhl C (2000) MRI of breast tumors. European Journal of Radiology 10: 46-58.

4. Hayes C, Padhani A, Leach M (2002) Assessing changes in tumour vascular function using dynamic contrast-enhanced magnetic resonance imaging. NMR in Biomedicine 15: 154-63.

5. Gilles R, Guinebretiere JM, Lucidarme O, Cluzel P, Janaud G, et al. (1994) Nonpalpable breast tumors: diagnosis with contrast-enhanced subtraction dynamic MR imaging. Radiology 191: 625-31.

6. Hulka CA, Smith BL, Sgroi DC, Tan L, Edmister WB, et al. (1995) Benign and malignant breast lesions: differentiation with echo-planar MR imaging. Radiology 197: 33-8.

7. Kelcz F, Santyr GE, Cron GO, Mongin SJ (1996) Application of a quantitative model to differentiate benign from malignant breast lesions detected by dynamic, gadolinium-enhanced MRI. Journal of Magnetic Resonance Imaging 6: 743-52.

8. Kuhl CK, Mielcareck P, Klaschik S, Leutner C, Wardelmann E, et al. (1999) Dynamic breast MR imaging: are signal intensity time course data useful for differential diagnosis of enhancing lesions? Radiology 211: 101.

9. Nunes LW, Schnall MD, Orel SG, Hochman MG, Langlotz CP, et al. (1997) Breast MR imaging: interpretation model. Radiology 202: 833-41.

10. Perman WH, Heiberg EM, Grunz J, Herrmann VM, Janney CG (1994) A fast 3D-imaging technique for performing dynamic Gd-enhanced MRI of breast lesions. Magnetic Resonance Imaging 12: 545-51.

11. Fischer U, Kopka L, Brinck U, Korabiowska M, Schauer A, et al. (1997) Prognostic value of contrast enhanced MR mammography in patients with breast cancer. Eur Radiology 10.1007/s003300050240.

12. Planey CR, Welch EB, Xu L, Chakravarthy AB, Gatenby JC, et al. (2009) Temporal sampling requirements for reference region modeling of DCE-MRI data in human breast cancer. Journal of Magnetic Resonance Imaging 30: 121-34.

13. Sung K, Daniel BL, Hargreaves BA (2013) Transmit B1+ field inhomogeneity and T1 estimation errors in breast DCE-MRI at 3 Tesla. Journal of Magnetic Resonance Imaging 38: 454-9.

14. Azlan CA, Di Giovanni P, Ahearn TS, Semple SI, Gilbert FJ, et al. (2010) B1 transmission-field inhomogeneity and enhancement ratio errors in dynamic contrast-enhanced MRI (DCE-MRI) of the breast at 3T. Journal of Magnetic Resonance Imaging 31: 234-9.

15. Kuhl CK, Kooijman H, Gieseke J, Schild HH (2007) Effect of B1 inhomogeneity on breast MR imaging at 3.0 T. Radiology 244: 929-30.

16. Profile (2020): DCE MRI Quantification. Quantitative Imaging Biomarkers Alliance.

17. Tsai WC, Kao KJ, Chang KM, Hung C, Yang Q, et al. (2017) B1 Field correction of T1 estimation should be considered for Breast Dynamic contrast-enhanced MR imaging even at 1.5 T1. Radiology 282: 55-62.

18. Bedair R, Graves MJ, Patterson AJ, McLean MA, Manavaki R, et al. (2016) Effect of radiofrequency Transmit Field correction on Quantitative Dynamic contrast enhanced MR imaging of the Breast at 3.0 T. Radiology 279: 368-77.

19. Pineda FD, Medved M, Fan X, Karczmar GS (2016) B1 and T1 mapping of the breast with a reference tissue method. Magnetic Resonance Medicine 75: 1565-73.

20. Van Schie JJ, Lavini C, Van Vliet LJ, Vos FM (2015) Feasibility of a fast method for B1- Inhomogeneity correction for FSPGR sequences. Magnetic Resonance Imaging 33: 312-8.

21. Jena A, Taneja S, Singh A, Negi P, Mehta SB, et al. (2017) Role of pharmacokinetic parameters derived with high temporal resolution DCE MRI using simultaneous PET/MRI system in breast cancer: A feasibility study. European Journal of Radiology 86: 261-6.

22. Jena A, Mehta SB, Taneja S (2013) Optimizing MRI Scan Time in the Computation of Pharmacokinetic Parameters (Ktrans) in Breast Cancer Diagnosis. Journal of Magnetic Resonance Imaging 38: 573-9.

23. Brookes AJ, Redpath TW, Gilbert FJ, Murray AD, Staff RT (1999) Accuracy of T1 measurement in dynamic contrast-enhanced breast MRI using two and three dimensional variable flip angle fast low angle shot. Journal of Magnetic Resonance Imaging 9: 163-71.

24. Rahbar H, Partridge SC, DeMartini WB, Thursten B, Lehman CD (2013). Clinical and technical considerations for high quality breast MRI at 3 Tesla. Journal of Magnetic Resonance Imaging 37: 778-90.

25. Hancu I, Lee SK, Dixon WT, Sacolick L, Becerra R, et al. (2012) Field shaping arrays: a means to address shading in high field breast MRI. Journal of Magnetic Resonance Imaging 36: 865-72.

26. Keenan KE, Wilmes LJ, AliuSO, Newitt DC, Jones EF, et al. (2016) Design of a Breast Phantom for Quantitative Magnetic Resonance Imaging. Journal of Magnetic Resonance Imaging 44: 610-9.

27. Sung K, Saranathan M, Daniel BL, Hargreaves BA (2013). Simultaneous T1 and B1 + mapping using reference region variable flip angle imaging. Magnetic Resonance Medicine 70: 954-61.

28. Rakow-Penner R, Daniel B, Yu H, Sawyer-Glover A, Glover GH (2006). Relaxation times of breast tissue at 1. 5T and 3T measured using IDEAL. Journal of Magnetic Resonance Imaging 3: 87-91.

29. Edden RAE, Smith SA (2010) Longitudinal and Multi-Echo Transverse Relaxation Times of Normal Breast Tissue at 3 Tesla. Journal of Magnetic Resonance Imaging 32: 982-7.